1   **Atmospheric Evolution of Emissions from a Boreal Forest Fire: The Formation of Highly-**

2   **Functionalized Oxygen-, Nitrogen-, and Sulfur-Containing Organic Compounds**

4   Jenna C. Ditto[1], Megan He[1], Tori N. Hass-Mitchell[1], Samar G. Moussa[2], Katherine Hayden[2],

5   Shao-Meng Li[2], John Liggio[2], Amy Leithead[2], Patrick Lee[2], Michael J. Wheeler[2],

6   Jeremy J.B. Wentzell[2], Drew R. Gentner[1,3,*]

8   [1] Department of Chemical and Environmental Engineering, Yale University, New Haven, CT,

9   06511, USA; [2] Air Quality Research Division, Environment and Climate Change Canada,

10 Toronto, Ontario M3H 5T4, Canada; [3] Solutions for Energy, Air, Climate and Health

11 (SEARCH), School of the Environment, Yale University, New Haven CT 0651, USA

13 * Correspondence to: drew.gentner@yale.edu

15 **Abstract**

16   Forest fires are major contributors of reactive gas- and particle-phase organic compounds

17 to the atmosphere. We used offline high resolution tandem mass spectrometry to perform a

18 molecular-level speciation of gas- and particle-phase compounds sampled via aircraft from an

19 evolving boreal forest fire smoke plume in Saskatchewan, Canada. We observed diverse

20 multifunctional compounds containing oxygen, nitrogen, and sulfur (CHONS), whose structures,

21 formation, and impacts are understudied. The dilution-corrected absolute ion abundance of

22 particle-phase CHONS compounds increased with plume age by a factor of 6.4 over the first 4

23 hours of downwind transport, and their relative contribution to the observed functionalized

organic aerosol (OA) mixture increased from 19% to 40%. The dilution-corrected absolute ion

abundance of particle-phase compounds with sulfide functional groups increased by a factor of

13 with plume age, and their relative contribution to observed OA increased from 4% to 40%.

Sulfides were present in up to 75% of CHONS compounds and the increases in sulfides were

accompanied by increases in ring-bound nitrogen; both increased together with CHONS

prevalence. A complex mixture of intermediate- and semi-volatile gas-phase organic sulfur

species was observed in emissions from the fire and depleted downwind, representing potential

precursors to particle-phase CHONS compounds. These results demonstrate CHONS formation

from nitrogen/oxygen-containing biomass burning emissions in the presence of reduced sulfur

species. In addition, they highlight chemical pathways that may also be relevant in situations

with elevated emissions of nitrogen- and sulfur-containing organic compounds from residential

biomass burning and fossil fuel use (e.g. coal), respectively.

1 Introduction

Forest fires are predicted to become increasingly prevalent and severe with climate

change (Abatzoglou and Williams, 2016; Barbero et al., 2015; Jolly et al., 2015). These fires are

an important and uncontrolled source of gas- and particle-phase compounds to the atmosphere,

including a complex mixture of gas-phase reactive organic carbon, primary organic aerosol

(POA), carbon monoxide, carbon dioxide, methane, ammonia, nitrogen oxides, and black carbon

(Akagi et al., 2011; Gilman et al., 2015; Hatch et al., 2015, 2018; Koss et al., 2018; Vicente et

al., 2013; Yokelson et al., 2013). Many of these emitted compounds are precursors to downwind

ozone and secondary organic aerosol (SOA) production (Ahern et al., 2019; Buysse et al., 2019;

Gilman et al., 2015; Hennigan et al., 2011; Lim et al., 2019).

47   Primary and secondary pollutants from biomass burning have important effects on air

48   quality locally, regionally, and continentally (Burgos et al., 2018; Colarco et al., 2004; Cottle et

49   al., 2014; Dreessen et al., 2016; Forster et al., 2001; Rogers et al., 2020; Val Martín et al., 2006),

50   and their impacts on human health and climate (e.g. via light absorbing brown and black carbon)

51   have been well documented (Forrister et al., 2015; Jiang et al., 2019; Liu et al., 2017; Di Lorenzo

52   et al., 2018; Reid et al., 2016; Sengupta et al., 2018; Wong et al., 2019). These health and climate

53   effects are sensitive to the elemental and structural composition of gas- and particle-phase

54   emissions and transformation products (Hallquist et al., 2009; Nozière et al., 2015). As a result,

55   past studies have used online and offline mass spectrometry techniques to characterize the

56   chemical composition of fresh and aged biomass burning emissions and have revealed a wide

57   array of emitted hydrocarbons and oxygen-, nitrogen-, or sulfur-containing functionalized

58   species (Ahern et al., 2019; Bertrand et al., 2018; Gilman et al., 2015; Hatch et al., 2015, 2018,

59   2019; Iinuma et al., 2010; Koss et al., 2018; Laskin et al., 2009; Yokelson et al., 2013).

60   However, the emissions and chemical transformations occurring in ambient biomass burning

61   plumes are extremely complex and despite previous measurements remain poorly understood at

62   the molecular-level.

63   In this study, we used an aircraft sampling system developed to collect offline gas- and

64   particle-phase organic compounds above a boreal forest fire. We examined the molecular-level

65   emissions and evolution of the forest fire plume via an analysis of these offline samples using

66   gas and liquid chromatography (GC/LC) with high resolution mass spectrometry (MS), including

67   tandem mass spectrometry (MS/MS). This degree of detailed chemical speciation is important to

68   advance knowledge of in-plume chemical pathways and reaction products, long-distance

69 transport, and fate of biomass burning products—all of which will improve modeling capabilities

70 and our understanding of the health and environmental impacts of biomass burning.

71   Specifically, the goals of this study were: (1) to perform a detailed speciation of gas- and

72 particle-phase organic compounds derived from the boreal forest fire in terms of elemental and

73 functional group composition, to assess changes in composition at the molecular-level as the

74 plume aged; and (2) to examine the evolution of oxygen-, nitrogen-, and sulfur-containing

75 (CHONS) compounds. These CHONS compounds made up 19-40% of functionalized OA here

76 and have been observed at other ambient sites (e.g. 9-11% (Ditto et al., 2018)), though little is

77 known about their structures or formation mechanisms. Using our observations of gas-phase

78 sulfur species, we identified possible precursors and reaction pathways involved in the formation

79 of these CHONS compounds.

80

81   **2   Materials and Methods**

82   On June 25th, 2018, two research flights were conducted by Environment and

83 Climate Change Canada as part of their Air Pollution research program. These flights sampled

84 two boreal wildfire smoke plumes originating near Lac La Loche in northern Saskatchewan,

85 Canada (Figure S1). The region is dominated by pine and spruce trees (Canada's National Forest

86 Inventory, 2020). Gas- and particle-phase samples were collected from the National Research

87 Council of Canada's Convair-580 research aircraft for analysis with offline high resolution mass

88 spectrometry, alongside many other measurements (Supporting Information S1-S2). The aircraft

89 flew the same straight-line tracks at multiple altitudes through the smoke plumes (average

90 altitudes shown in Table S1), which when stacked created a virtual screen intercepting the

91 plumes at each of five downwind locations (with flight design similar to those previously

92 reported (Li et al., 2017; Liggio et al., 2016)). Screen 1 was ~10 km from the fire with screens 2-

93 4 following the plumes downwind, and screen 5 intercepting the plumes after they had passed

94 over several major surface and in-situ mining oil sands facilities (Figure S1). The samples

95 discussed here were collected across both plumes to ensure that enough mass was present to well

96 surpass the mass spectrometer's detection limits. Based on satellite information and aircraft

97 measurements at the start of sampling (i.e. screen 1), the fire was a low-intensity surface fire

98 with smoldering conditions; aircraft measurements indicated a modified combustion efficiency

99 of 0.90±0.01 for both plumes.

100 Combined gas- and particle-phase samples were collected onto custom adsorbent tubes

101 packed with high-purity quartz wool, glass beads, Tenax TA, and Carbopack X (Sheu et al.,

102 2018). Samples were collected along screens 1-4 in Figure S1 (no adsorbent tubes collected at

103 screen 5) via an external pod mounted under the wing of the aircraft, which included remote

104 switching between adsorbent tubes at various transect altitudes and online measurements of

105 temperature, pressure, and flow (Supporting Information S1, Figure S2).

106 All adsorbent tubes were analyzed using a GERSTEL Thermal Desorber TD 3.5+ with

107 gas chromatography (Agilent 7890B GC), atmospheric pressure chemical ionization (APCI), and

108 quadrupole time-of-flight mass spectrometry (Agilent 6550 Q-TOF), similar to past work (Khare

109 et al., 2019). For adsorbent tubes, the APCI was operated in positive ionization mode and the Q-

110 TOF was operated in MS mode (i.e. TOF data collection only, hereafter "GC-APCI-MS").

111 Adsorbent tube data were processed primarily via a targeted approach for C_xH_y, $C_xH_yO_1$, $C_xH_yS_1$,

112 and $C_xH_yN_1$ compounds using custom Igor Pro code (Supporting Information S2-S3).

113 In order to reduce losses of lower volatility gases onto upstream surfaces, particles were

114 not explicitly filtered out at the inlet of the wing-pod sampler used for adsorbent tube collection.

115   For several reasons, it was concluded that the C_xH_y hydrocarbons smaller than C_{22-23} (and

116     $C_xH_yS_1/C_xH_yO_1/C_xH_yN_1$ compounds of similar volatility) measured in the adsorbent tubes were

117   predominantly in the gas-phase. This was based on (1) significant undersampling for particles at

118   the wing pod inlet since the adsorbent tube sampling flow rate was a factor of ~4 lower than its

119   corresponding isokinetic flow rate, resulting in a significant divergence of particles away from

120   the inlet during sampling; and (2) partitioning theory, using average in-plume organic aerosol

121   (OA) concentrations of 18-22 $\mu g/m^3$ across adsorbent tube sampling periods for screens 1-4,

122   concurrently measured by an aerosol mass spectrometer (AMS) onboard the aircraft (see

123   Supporting Information S1, S3, Table S2). Thus, the C_{22} and smaller C_xH_y compounds (and other

124   compound classes of similar volatility) should have primarily been in the gas phase at

125   equilibrium. As such, we limited the following adsorbent tube data analysis to compounds in the

126   C_{10}-C_{25} range to focus on intermediate-volatility and semivolatile (I/SVOCs) compounds present

127   in the gas phase. In our analyses and interpretation, the compounds included in each of these

128   volatility ranges are defined based on fixed values of saturation mass concentrations (e.g.

129   Donahue et al., 2011; Murphy et al., 2014) at the observed 18-22 ug/m^3 OA loadings present

130   during adsorbent tube sampling times.

131   Dedicated particle-phase samples were collected on 47 mm PTFE filters (2.0 μm pore;

132   Pall Corporation) from a sampling manifold in the aircraft cabin containing six independent

133   anodized aluminum filter holders. The filters were sampled behind an isokinetic inlet with a size

134   cutoff of approximately 2.5 μm. One filter sample was collected per screen for screens 1-5

135   shown in Figure S1.

136   Filter samples were extracted in methanol (Ditto et al., 2018). Samples were analyzed via

137   liquid chromatography (Agilent 1260 LC) with electrospray ionization (ESI) and the same Q-

138   TOF. For filters, the ESI source was operated in both positive and negative ionization modes,

139   and the Q-TOF was operated in both MS mode (i.e. TOF data collection, "LC-ESI-MS") and

140   MS/MS mode (i.e. tandem mass spectral data collection, "LC-ESI-MS/MS") (Ditto et al., 2018,

141   2020). Filter extracts were also analyzed using GC-APCI-MS in positive ionization mode. Filter

142   data from LC-ESI-MS, LC-ESI-MS/MS, and GC-APCI-MS were analyzed with a non-targeted

143   approach, using Agilent Mass Hunter, SIRIUS with CSI:FingerID, and custom R code

144   (Supporting Information S2-S3) (Ditto et al., 2018, 2020). All peaks that passed strict QA/QC

145   (Section S3) were assigned molecular formulas, with candidate formulas limited to 20 oxygen, 3

146   nitrogen, and/or 1 sulfur atom(s). Hereafter, LC-ESI compound classes are discussed here

147   without subscripts.

148   The particle-phase compounds observed via LC-ESI vs. GC-APCI techniques varied

149   significantly in their oxygen, nitrogen, and sulfur content since these two chromatographic and

150   ionization approaches are sensitive towards different types of compounds (see Section S5). As

151   the forest fire plume aged, the complex mixture of emissions and secondary products became

152   increasingly functionalized and thus less GC-amenable without derivatization. Therefore, we

153   focused on LC-ESI-MS data to study these functionalized particle-phase compounds. We

154   acknowledge that this method excludes fully-reduced hydrocarbons and fully-reduced sulfur-

155   containing particle-phase compounds (i.e. CH and CHS (Ditto et al., 2018)) and thus these

156   compound classes are not accounted for in the relative particle-phase distributions shown here.

157   For particle-phase analyses, we estimated saturation mass concentration based on the Li

158   et al. parameterization (Li et al., 2016), then grouped compounds based on fixed volatility bins

159   (Donahue et al., 2011; Murphy et al., 2014). Particle-phase compounds were observed across the

160   IVOC, SVOC, LVOC, and ELVOC ranges. Particle-phase IVOCs have been observed in the

161 past, and despite their higher volatility, may exist in the particle-phase due to their polarity and

162 water solubility. Additional details on these methods, including a discussion of total mass

163 analyzed from filters/adsorbent tubes and QA/QC, are discussed in Supporting Information S1-

164 S5, with a methods summary shown in Figure S3.

165

166 **3   Results**

167   3.1 Evolution of organic aerosol elemental composition and functionality with plume age

168   Our analysis of functionalized OA showed several compositional trends in the evolving

169 boreal forest fire smoke plume (screens 1-4) and exhibited marked changes after emissions from

170 the oil sands facilities were mixed with the forest fire plume (screen 5). Here, we focused on the

171 forest fire plume in screens 1-4. We observed a diverse elemental composition in functionalized

172 OA across oxygen-, nitrogen-, and/or sulfur-containing compound classes (Figure 1A-1B, Figure

173 S5). This included oxygenates (CHO), such as common biomass burning tracers and their

174 isomers (e.g. levoglucosan, Supporting Information S2); as well as oxygen- and nitrogen-

175 containing compounds (CHON); oxygen- and sulfur-containing compounds (CHOS); reduced

176 nitrogen-containing compounds (CHN); reduced nitrogen- and sulfur-containing compounds

177 (CHNS); as well as compounds containing oxygen, nitrogen, and sulfur (CHONS).

178   There was a continual decrease in the relative abundance of particle-phase CHO

179 compounds in the observed functionalized OA across screens 1-4, accompanied by a consistent

180 relative increase in CHON and CHONS compounds (Figure 1B). Notably, the relative abundance

181 of CHONS compounds increased from 19% to 40% of measured functionalized OA from screens

182 1 to 4. Trends in absolute ion abundances were also similar (note: carbon monoxide mixing ratio

183 was used to account for dilution). This is shown in Figure 1C (inset) and Figure S5C; CHO

184   generally decreased from screens 1 to 4, while CHONS and CHON generally increased,

185   suggesting that CHONS compounds were possibly formed from CHO, CHN, and/or CHON

186   precursors in the gas- and/or particle-phases. Specifically, the dilution-corrected abundance of

187   CHONS species increased by a factor of 6.4 from screen 1 to 4 (Figure 1C, inset). In Figure 1,

188   we primarily presented data as relative contributions to functionalized OA to examine changes in

189   the evolution of the complex mixture as a whole and the relationships between different

190   compound classes and functional groups with plume age. However, dilution-corrected

191   abundances are also important for understanding absolute formation (or depletion), and are

192   shown for all species in Figures S5-S6.

193   Based on MS/MS analyses, these evolving CHO, CHN, CHON, and CHONS compounds

194   were often comprised of variable combinations of hydroxyl and ether functional groups (e.g.

195   primary emissions from forest fires like methoxyphenols and similar structures), as well as

196   amine, imine, and sulfide groups, along with cyclic nitrogen structural features (consistent with

197   past laboratory observations of biomass burning emissions (Laskin et al., 2009; Lin et al., 2018;

198   Liu et al., 2015; Updyke et al., 2012)).

199

200   3.2 Detailed speciation of CHONS compounds in functionalized OA

201   While some individual CHONS species contained grouped oxygen, nitrogen, and sulfur

202   atom moieties (e.g. sulfonamides), the majority of CHONS compounds had a combination of

203   multiple separate oxygen-, nitrogen-, and/or sulfur-containing functional groups (Figure 2A-2B).

204   Sulfide groups were important contributors to CHONS compounds (Figure 2B) and showed a

205   notable increase in relative contribution to the overall functional group distribution with plume

206   age (Figure 1C). They increased from 4% to 40% of measured compound abundance across

207   screens 1 to 4 (Figure 1C), which corresponded to an increase by a factor of 13 in terms of their

208   dilution-corrected abundance (Figure 1C, inset). Their increasing relative contribution to

209   CHONS compounds with plume evolution was even more pronounced—by screen 4, the sulfide

210   functional group was present in 75% of detected CHONS compound abundance (Figure S7A).

211   Here, we focused on the presence of sulfides in CHONS compounds because most of the

212   observed particle-phase sulfides occurred as part of CHONS species (71%), while a smaller

213   fraction occurred in CHOS (21%) or CHNS (8%) compounds (Figure 3A).

214   To explore possible precursors and formation pathways for these particle-phase sulfide-

215   containing CHONS species, we used MS/MS to identify nitrogen-containing functional groups

216   that co-occurred with sulfides. In CHONS compounds, most sulfides co-occurred with cyclic

217   nitrogen (36% of sulfide-containing species), amine (32%), or imine features (43%) (Figure 3B).

218   The prevalence of sulfide and cyclic nitrogen features in the measured functionalized OA

219   increased together screen-to-screen, and increased together with the rising proportion of CHONS

220   compounds (Figure 3C). While sulfides often co-occurred with amines or imines and while

221   amines and imines were prevalent in all 4 screens (Figure 1C), there was no relationship between

222   these functional groups and the increasing contribution of CHONS compounds to measured

223   functionalized OA (Figure S7B).

224   The sulfide substructures observed via MS/MS often contained linear carbon chains or

225   phenyl groups bonded to the sulfur atom (Figure 3C inset). Thus, we hypothesize that precursors

226   with similar reduced sulfur-containing structures reacted with cyclic nitrogen-containing species

227   to form the observed particle-phase sulfide-containing CHONS compounds (see further

228   discussion of possible precursors in Section 3.3, and potential chemical pathways in Section 4.2).

229   CHONS compounds were predominantly SVOCs in screens 1-4 (i.e. 89% of CHONS ion

230   abundance, Figure 2C, Figure S8), suggesting that these compounds were formed from higher

231   volatility gas-phase species. In contrast, with the added influence of the oil sands facilities in

232   screen 5, 68% of CHONS compounds were extremely low volatility organic compounds

233   (ELVOCs), though CHONS made up only 2% of functionalized OA at screen 5.

234   Overall, dilution-corrected abundances of functionalized OA in each particle-phase

235   volatility bin increased with plume age, but the relative contribution of SVOCs increased from

236   37% to 58% while the relative contribution of IVOCs dropped from 38% to 20%, potentially due

237   to oxidation reactions that formed SVOCs and/or due to evaporation (Figure S9). These particle-

238   phase IVOCs consisted predominantly of CHO, CHN, and CHON (O/N < 3) compounds, which

239   could include possible non-sulfur containing precursors to the observed CHONS species.

240   Fragmentation of particle-phase L/ELVOC compounds also could have contributed to some of

241   the observed SVOC mass, but the overall increasing total abundance across all volatility bins

242   with plume age supports the idea that these compounds were predominantly formed from more

243   volatile precursors (e.g. I/SVOCs).

244

245   3.3 Targeted search for CHONS precursors in the gas-phase

246   To investigate the precursors and chemistry that could have formed the sulfide-containing

247   CHONS species observed in the particle-phase samples, we performed a targeted search for

248   possible gas-phase I/SVOC species in each adsorbent tube, across all C_{10}-C_{25} $C_xH_yS_1$ species

249   with the equivalent of 0-15 double bonds and/or rings (i.e. $C_xH_{2x+2}S_1$- $C_xH_{2x-28}S_1$, Figure 4A,

250   Figure S10). We observed a distribution of $C_xH_yS_1$ compounds and their isomers; based on the

251   high mass resolution and high mass accuracy molecular formulas from targeted GC-APCI-MS

252   analysis, 27% of $C_xH_yS_1$ compounds were fully saturated (i.e. $C_xH_{2x+2}S_1$) and 25% contained the

253   equivalent of 4-6 double bonds and/or rings (i.e. $C_xH_{2x-6}S_1$- $C_xH_{2x-10}S_1$), which included single

254   ring aromatics. We focused on these sulfur-containing gases as candidate precursors to the

255   observed particle-phase sulfide-containing CHONS compounds as they contained sulfur

256   substructures with linear carbon chains or phenyl groups, similar to those observed on particle-

257   phase CHONS compounds via MS/MS analysis (Figure 3C inset, Figures S10-S11). However,

258   we also observed contributions from other sulfur-containing structures (e.g. with the equivalent

259   of 1-3 double bonds and/or rings, Figure 4A), which could also have been precursor species.

260   The observed gas-phase C_{10}-C_{25} $C_xH_yS_1$ compounds were present in gas-phase emissions

261   from the fire and likely also evaporated from primary OA during early plume dilution. Gas-phase

262   C_{10}-C_{25} $C_xH_yS_1$ concentrations increased relative to carbon monoxide from screen 1 to 2, then

263   steadily decreased with plume age (Figure 4B, Figure S12A). This suggests the gas-phase

264   emission and/or evaporation of $C_xH_yS_1$ compounds from OA between screens 1 and 2, and

265   subsequent participation in plume chemistry from screens 2 to 4.

266   Similar OA evaporation with plume dilution has been observed in many past studies

267   (Ahern et al., 2019; Garofalo et al., 2019; Hennigan et al., 2011; Lim et al., 2019). To better

268   understand the dynamics of these sulfur-containing compounds and their possible particle-phase

269   origin, we compared their concentrations to those of C_{10}-C_{25} aliphatic and aromatic C_xH_y and

270    $C_xH_yO_1$ species from a similar targeted search of adsorbent tube gas-phase compounds. Overall,

271   C_xH_y and $C_xH_yO_1$ compound classes dominated the observed C_{10}-C_{25} compounds (Figure 4B,

272   Figure S12B), with 61% C_xH_y, 36% $C_xH_yO_1$, and just 3% $C_xH_yS_1$ on average. C_xH_y and $C_xH_yO_1$

273   concentrations generally increased with plume age (Figure 4B) and included many known

274   compound types (e.g. monoterpenes, aromatics, hydroxyls, carbonyls (Akagi et al., 2011;

275   Andreae, 2019; Gilman et al., 2015; Hatch et al., 2015, 2019; Koss et al., 2018)). This suggests

276   the direct emission of these gas-phase compound classes from the fire (observed at screen 1)

277   along with the evaporation of semivolatile particle-phase emissions as the plume evolved, and

278   formation of $C_xH_yO_1$ via C_xH_y oxidation. AMS measurements of total OA concentrations

279   provided supporting evidence of OA evaporation; the ratio of AMS OA concentration to CO

280   decreased by 7% from screen 1 to 2 (corresponding to an AMS OA/CO ratio of -0.0044 or a

281   decrease in OA concentrations of -2.3 µg/m^3), while the ratio of total gas-phase C_xH_y, $C_xH_yO_1$,

282   and $C_xH_yS_1$ concentration to CO increased by 55% (corresponding to a total gas-phase

283   concentration/CO ratio of 0.022 or an increase in gas-phase concentration of 7.0 µg/m^3, with

284   changes summarized in Table S3). While not the focus of the analytical approaches applied in

285   this study, to further substantiate the observation of OA evaporation, we performed the same

286   targeted analysis of C_{10}-C_{25} C_xH_y, $C_xH_yO_1$, and $C_xH_yS_1$ compounds in the particle-phase filter

287   sample extracts analyzed via GC-APCI-MS. We observed a similar decrease in concentration

288   from screen 1 to 2. However, these filter measurements (even with APCI ionization) were not

289   geared towards C_xH_y and $C_xH_yS_1$ speciation due to possible solubility limitations in the

290   extraction solvent (Supporting Information S4). Direct thermal desorption of quartz filters with

291   GC-APCI analysis would be better suited for these C_xH_y and $C_xH_yS_1$ measurements (as

292   performed in this study with adsorbent tubes).

293   As discussed in *Materials and Methods*, the observed compounds with volatilities below

294   that of ~C_{22}-C_{23} hydrocarbons existed primarily in the gas-phase (Table S2), while larger

295   compounds favored the particle-phase (with a smaller fraction in the gas-phase at equilibrium).

296   The presence of gas-phase compounds across this I/SVOC range (e.g. Figures S10, S13) further

297   corroborates the possibility of contributions from both direct gas-phase emissions and from

298 evaporation of particle-phase emissions (Supporting Information S3). In contrast to C_xH_y

299 concentrations, $C_xH_yS_1$ concentrations dropped markedly after screen 2 despite similarities in the

300 volatility distribution of C_xH_y and $C_xH_yS_1$ I/SVOC mixtures (Figure 4A, Figures S10 and S13).

301 This difference across screens shows that the observed $C_xH_yS_1$ I/SVOCs were removed (e.g. via

302 chemical reactions) more quickly than C_xH_y (Figure 4B), thus supporting their potential

303 contribution to CHONS formation.

304   In addition to the C_{10}-C_{25} $C_xH_yS_1$ compounds measured in the adsorbent tubes, smaller

305 sulfur-containing compounds could have also acted as CHONS precursors, like those identified

306 by the onboard proton transfer reaction-mass spectrometer (PTR-ToF-MS). While dimethyl

307 sulfide (DMS, previously observed in biomass burning smoke (Andreae, 2019)) was often below

308 the instrument's limit of detection, both dimethyl and diethyl sulfide showed good correlation

309 with acetonitrile (a well-known biomass burning product (Andreae, 2019)) in the smoke plume

310 during screen 1 (r ~ 0.95, Figure S12C). This suggests that these compounds were co-emitted by

311 the fire.

312

313 **4 Discussion**

314 4.1 Investigating possible origins of gas-phase sulfur compounds

315   The gas-phase sulfur-containing compounds observed in the plume were emitted from the

316 smoldering fire. However, their origins are uncertain, since the broader range of sulfur species

317 found here (Figure 4A, Figures S10-11) has not been previously reported; many of the

318 compounds in the complex mixture of sulfur-containing compounds discussed in this work were

319 outside the detection range of previously employed methods (Hatch et al., 2015; Khare et al.,

320 2019; Koss et al., 2018; Sekimoto et al., 2018). Here, we explore two potential origins of these

321   gas-phase sulfur-containing precursors to the observed particle-phase CHONS compounds: the

322   biomass fuel itself and the deposition of sulfur species from anthropogenic/industrial operations.

323   *Fuel:* In past studies, emissions of sulfur-containing organic compounds were typically

324   minor compared to-oxygen- or nitrogen-containing compounds, and the relative balance of

325   oxygen-, nitrogen-, or sulfur-containing compound emissions was typically proportional to fuel

326   content (Hatch et al., 2015; Ward, 1990). The estimated N:S ratio for boreal forest fuel near the

327   fire was ~10:1 (Huang and Schoenau, 1996), which was similar to the average N:S ratio from a

328   non-targeted search for nitrogen- and sulfur-containing I/SVOCs from the adsorbent tube

329   samples in this study of (8.1 ± 4.8):1. Sulfur is an essential nutrient in plants, and can be taken up

330   from soil (as sulfate) or from the atmosphere via deposition (as SO_2 and sulfate) (Aas et al.,

331   2019; Gahan and Schmalenberger, 2014; Leustek, 2002). Both SO_2 and sulfate are metabolized

332   in plants to yield a variety of compounds critical to plant functions including cysteine and a

333   range of other sulfur- (as well as oxygen- and nitrogen-) containing compounds (Leustek, 2002).

334   In addition, disulfide bonds contribute to plant protein structure, and these bonds can cleave and

335   form thiols (Gahan and Schmalenberger, 2014; Leustek, 2002; Onda, 2013). Sulfur-containing

336   compounds like these may have been emitted during the fire, along with other known sulfur

337   products from boreal fuels (e.g. DMS, thiophenes (Akagi et al., 2011; Hatch et al., 2015; Koss et

338   al., 2018; Landis et al., 2018)).

339   *Deposition:* While sulfur can be naturally occurring, it is also associated with

340   anthropogenic activities (e.g. transportation, power generation, industry, etc.). A portion of the

341   sulfur in the forest fire emissions could have originated from sulfur deposited via such

342   anthropogenic activities. The closest large anthropogenic sulfur source to the fire location was

343   the oil sands mining region north of Fort McMurray, Alberta, which was approximately 150 km

344 away and which contains known SO_2 emitters (Liggio et al., 2017; McLinden et al., 2016).

345 Regional concentrations of SO_2 or other sulfur species from these nearby industrial activities

346 could have led to accumulated deposition of inorganic and/or organic sulfur compounds over

347 time, though it is uncertain how much of this deposited sulfur would have been taken up and

348 transformed by vegetation due to sulfur uptake and assimilation regulatory pathways in plants

349 (Davidian and Kopriva, 2010). This possible accumulated deposition may have acted as a

350 reservoir of sulfur to be emitted during fires via the re-volatilization of deposited compounds, in

351 addition to the evaporation of typical sulfur metabolites or the formation of sulfur-containing

352 combustion by-products. This hypothesis is consistent with recent deposition measurement and

353 modeling results for the region, which indicated that sulfur deposition from the oil sands

354 operations potentially impacted areas downwind, including the region where this fire occurred

355 (Makar et al., 2018).

356   Interestingly, lichen and spruce trees, which are prominent in the region of the fire

357 discussed here, have been reported to accumulate sulfur from SO_2 in regions near large industrial

358 SO_2 sources (Meng et al., 1995; Nyborg et al., 1991). Also, past studies have reported

359 enhancements in sulfate (as well as nitrate/ammonium) aerosols coming from biomass burning in

360 areas with urban influence (Fenn et al., 2015; Hecobian et al., 2011; Hegg et al., 1987).

361 Inorganic aerosol components from both urban (e.g. Edmonton, Alberta) and industrial (e.g. oil

362 sands) sources could deposit in the area surrounding the emissions source along with an organic

363 phase, which we postulate could contain a range of sulfur-containing species including the

364 $C_xH_yS_1$ compounds shown here. These deposited inorganic and organic species may have re-

365 volatilized during the fire. However, further work is needed to disentangle the contribution of

366 natural vs. anthropogenic sulfur to biomass burning emissions in the region. Also, we note that

367   the fire was ~1 hour old at the time of sampling, so the recent application of fire suppressants

368   was unlikely to contribute to the species observed.

369

370   4.2 Potential reaction pathways leading to sulfides in CHONS from sulfur precursors

371   A number of potential reactions involving sulfur-containing precursors, often thiols (R-

372   SH), may have contributed to the formation of the observed sulfide functional groups in particle-

373   phase CHONS compounds (Figure S14). On average, our gas-phase measurements were

374   comprised of 27% fully saturated sulfur-containing hydrocarbons (i.e. $C_xH_{2x+2}S_1$, Figures S10-

375   11). It is likely that some fraction of the sulfur compounds observed in the gas-phase adsorbent

376   tube measurements (e.g. the compounds identified as $C_xH_{2x+2}S_1$) and in PTR-ToF-MS

377   measurements (e.g. dimethyl sulfide, diethyl sulfide) were thiols, but the distinction between

378   sulfide vs. thiol isomers was challenging with these methods without specific internal standards.

379   In some of the following possible reactions, a thiol interacts with a non-sulfur precursor

380   to yield a sulfide-containing compound. The non-sulfur precursor (in the gas- or particle-phase)

381   may have contained O and N atoms, thus yielding a CHONS compound immediately after

382   participating in one of the proposed reactions. Alternatively, the newly formed sulfide-containing

383   compound may have undergone subsequent, separate reactions with oxygen- and/or nitrogen-

384   containing species (in the gas- or particle-phase) to form the observed sulfide-containing

385   CHONS species. Here, we focused on possible reactions that could have contributed the sulfide

386   group to these oxygen- and/or nitrogen-containing compounds (known emissions from forest

387   fires, as discussed above). Earlier, we postulated that because most of the observed particle-

388   phase CHONS compounds were SVOCs, these compounds were predominantly formed by

389   reactions with more volatile gas-phase compounds. However, it is uncertain whether these

390   sulfide-forming and CHONS-forming reactions all occurred in the gas-phase with subsequent

391   partitioning to the particle-phase, heterogeneously, or in a combination of separate gas- and

392   particle-phase chemistry. We suggest some possible sulfide-forming reactions here, yet we note

393   that these proposed reactions are likely not comprehensive. Further work to elucidate the

394   chemistry driving this sulfide and CHONS formation is needed.

395   Some possible reactions include: (1) thiol-ene reactions, where a thiol reacts with an

396   alkene (or alkyne), which can form carbon-sulfur bonds (Lowe, 2010). Alkenes are known to be

397   prominent in emissions from boreal fires (Gilman et al., 2015; Hatch et al., 2015), and we

398   observed similar structures in our gas-phase samples that likely included alkenes, cyclic alkanes,

399   and/or monoterpenes (Figure S13). (2) Thiol reactions with carbonyls, which can form

400   hemithioacetals that subsequently dehydrate in the atmosphere to yield sulfides (Jencks and

401   Lienhard, 1966). This reaction is similar to the formation of enamines from carbonyls and

402   dimethyl amine via the formation and subsequent dehydration of a carbinolamine, which has

403   been shown to occur in ambient conditions (Duporté et al., 2016, 2017). (3) Thiol reactions with

404   alcohols, which can form sulfides; these reaction rates are low in the absence of catalysts and

405   require relatively high temperature to occur (i.e. 200-450°C (Mashkina, 1991), temperatures that

406   are relevant very close to the fire but unlikely in the cooled plume). (4) Another possibility is that

407   a radical intermediate product formed during atmospheric oxidation of DMS (e.g. the

408   methylthiomethyl radical ($CH_3SCH_2^{\bullet}$) from $OH^{\bullet}$-driven hydrogen abstraction of DMS (Barnes et

409   al., 2006)) interacted with CHN and CHON precursors to yield the observed sulfide-containing

410   CHONS products. However, the concentrations of the methylthiomethyl radical and similar

411   radicals from other small sulfide precursors would likely be lower than those of other major

412 drivers of in-plume radical chemistry (e.g. O_2, NO_x, etc.), thus making this reaction pathway less

413 likely to contribute.

414   Based on our observations of these sulfide-containing products across flight screens, the

415 overall timescale for these sulfide-forming reactions was likely approximately 1 hour (or less).

416 For the literature reactions referenced above, reaction timescales ranged from minutes to hours in

417 laboratory experiments, but extrapolation to rates in an ambient wildfire plume is uncertain.

418 Specifically, it is challenging to compare to predicted timescales for the proposed reactions

419 without knowing the exact structure/identities of the reactants or the possible role of other key

420 modifying factors in the plume (e.g. aerosol pH, presence of water).

421

422 **5   Implications and Conclusions**

423   In this work, we performed the first high resolution tandem mass spectrometry analysis of

424 an evolving plume from a smoldering boreal forest fire. The results show clear evidence of gas-

425 phase sulfur-containing emissions from the fire, and an increasing contribution from particle-

426 phase CHONS compounds with sulfide functional groups as the plume evolved. Together, these

427 results suggest the emission of gas-phase sulfur-containing compounds from the fire and

428 subsequent gas- and/or particle-phase chemistry that produced multifunctional sulfide-containing

429 CHONS compounds.

430   Sulfide functional groups in ambient air have been reported at a range of U.S. locations

431 from urban inland (1-7% sulfides), urban coastal (5-12% sulfides), and remote forested (7%

432 sulfides), and on average, sulfides comprised 28% of sulfur-containing functional groups at these

433 sites (Ditto et al., 2020). However, in past work, 53% of these sulfides were present in CHOS

434 compounds, while 34% were CHONS, and 13% were CHNS (in contrast to 21%, 71%, and 8%

435   in this study, respectively). Notably, at a Northeastern U.S. coastal site where there were several

436   pollution events linked to long distance transport of biomass burning smoke during field

437   sampling (Rogers et al., 2020), 70-90% of sulfides were present in CHONS compounds (Ditto et

438   al., 2020), similar to the compound class distribution of sulfides discussed here (Figure 3A).

439   These results, along with past observations, highlight that this type of chemistry and these

440   types of reaction products may be relevant to other regions where concentrations of nitrogen and

441   sulfur-containing precursors are high, such as in developing regions, emerging economies, or

442   megacities where residential biomass burning is common and coincident with extensive use of

443   sulfur-containing fossil fuels (e.g. coal). CHONS compounds have been reported in similar

444   regions in past studies (Lin et al., 2012; Pan et al., 2013; Song et al., 2019; Wang et al., 2017a,

445   2016, 2017b). Their formation is potentially important since the presence of sulfur, oxygen, and

446   nitrogen atoms in organic compounds can affect particle phase state (e.g. solid, semi-solid,

447   liquid), and mixing state (e.g. well-mixed, phase-separated) (DeRieux et al., 2018; Ditto et al.,

448   2019; Van Krevelen and Te Nijenhuis, 2009). These physical properties may influence particles'

449   chemical reactivity and overall persistence in the atmosphere, all of which contribute to the

450   health and environmental impacts that communities and ecosystems experience from OA

451   exposure. Future work to identify prominent functional groups in CHONS species in regions

452   with high CHONS concentrations will help elucidate the formation chemistry of these

453   functionalized compounds and understand and mitigate their associated impacts.

454

455

456

457

Acknowledgments

The authors acknowledge GERSTEL for their collaboration with the TDU 3.5+ used to run the GC-APCI adsorbent tubes and filters discussed in this study. We thank Environment and Climate Change Canada and National Research Council technical teams for their help in the construction and maintenance of cartridge sampling systems, specifically Tak Chan (Environment and Climate Change Canada) for help collecting samples. We also thank Jo Machesky (Yale) for help running adsorbent tube samples, Joe Lybik (Yale) for help packing adsorbent tubes, and Daniel Thompson (Natural Resources Canada) for informative discussion. J.C.D., M.H., T.H-M., and D.R.G. acknowledge support from National Science Foundation grant AWD0001666. We also acknowledge funding from the Air Pollution (AP) program of Environment and Climate Change Canada. The flights discussed in this study were embedded within a 2018 oil sands monitoring intensive campaign, and the oil sands monitoring program is acknowledged for enabling the flights.

Author Contributions

J.C.D. ran samples, processed filter data, compiled and interpreted results. M.H. processed adsorbent tube data. T.H-M. contributed to MS/MS analysis. S.G.M., K.H., J.L., and D.R.G. collaborated on data interpretation. K.H. collected and processed AMS data. A.L. collected and processed PTR-ToF-MS data. S.-M.L. designed the aircraft adsorbent tube collection system. P.L. and J.J.B.W. implemented the wing pod design. P.L. prepared the wing pods for collection and J.J.B.W. and J.L. collected the adsorbent tube samples. M.J.W. and J.L. designed the filter collection system. M.J.W. and K.H collected filter samples. S.-M.L., K.H., and J.L. designed the aircraft sampling study. J.C.D. and D.R.G. wrote the manuscript, with input from all co-authors.

481 **Competing Interests**

482 The authors declare that they have no conflicts of interest.

483

484 **Code and Data Availability**

485 Code and data are available upon request.

486

487 **References**

488 Aas, W., Mortier, A., Bowersox, V., Cherian, R., Faluvegi, G., Fagerli, H., Hand, J., Klimont, Z.,

489   Galy-Lacaux, C., Lehmann, C. M. B., Myhre, C. L., Myhre, G., Olivié, D., Sato, K.,

490   Quaas, J., Rao, P. S. P., Schulz, M., Shindell, D., Skeie, R. B., Stein, A., Takemura, T.,

491   Tsyro, S., Vet, R. and Xu, X.: Global and regional trends of atmospheric sulfur, Sci. Rep.,

492   9(1), 1–11, doi:10.1038/s41598-018-37304-0, 2019.

493 Abatzoglou, J. T. and Williams, A. P.: Impact of anthropogenic climate change on wildfire

494   across western US forests, Proc. Natl. Acad. Sci. U. S. A., 113(42), 11770–11775,

495   doi:10.1073/pnas.1607171113, 2016.

496 Ahern, A. T., Robinson, E. S., Tkacik, D. S., Saleh, R., Hatch, L. E., Barsanti, K. C., Stockwell,

497   C. E., Yokelson, R. J., Presto, A. A., Robinson, A. L., Sullivan, R. C. and Donahue, N.

498   M.: Production of Secondary Organic Aerosol During Aging of Biomass Burning Smoke

499   From Fresh Fuels and Its Relationship to VOC Precursors, J. Geophys. Res. Atmos.,

500   124(6), 3583–3606, doi:10.1029/2018JD029068, 2019.

501 Akagi, S. K., Yokelson, R. J., Wiedinmyer, C., Alvarado, M. J., Reid, J. S., Karl, T., Crounse, J.

502   D. and Wennberg, P. O.: Emission factors for open and domestic biomass burning for use

503   in atmospheric models, Atmos. Chem. Phys., 11(9), 4039–4072, doi:10.5194/acp-11-

504   4039-2011, 2011.

505   Andreae, M. O.: Emission of trace gases and aerosols from biomass burning – An updated

506   assessment, Atmos. Chem. Phys., 1–27, doi:10.5194/acp-2019-303, 2019.

507   Canada's National Forest Inventory, [online] Available from: https://nfi.nfis.org/en/ (Accessed

508   18 February 2020), 2020.

509   Barbero, R., Abatzoglou, J. T., Larkin, N. K., Kolden, C. A. and Stocks, B.: Climate change

510   presents increased potential for very large fires in the contiguous United States, Int. J.

511   Wildl. Fire, 24(7), 892–899, doi:10.1071/WF15083, 2015.

512   Barnes, I., Hjorth, J. and Mihalapoulos, N.: Dimethyl sulfide and dimethyl sulfoxide and their

513   oxidation in the atmosphere, Chem. Rev., 106(3), 940–975, doi:10.1021/cr020529+,

514   2006.

515   Bertrand, A., Stefenelli, G., Jen, C. N., Pieber, S. M., Bruns, E. A., Ni, H., Temime-Roussel, B.,

516   Slowik, J. G., Goldstein, A. H., Haddad, I. El, Baltensperger, U., Prévôt, A. S. H.,

517   Wortham, H. and Marchand, N.: Evolution of the chemical fingerprint of biomass

518   burning organic aerosol during aging, Atmos. Chem. Phys., 18(10), 7607–7624,

519   doi:10.5194/acp-18-7607-2018, 2018.

520   Burgos, M. A., Mateos, D., Cachorro, V. E., Toledano, C., de Frutos, A. M., Calle, A.,

521   Herguedas, A. and Marcos, J. L.: An analysis of high fine aerosol loading episodes in

522   north-central Spain in the summer 2013 - Impact of Canadian biomass burning episode

523   and local emissions, Atmos. Environ., doi:10.1016/j.atmosenv.2018.04.024, 2018.

524   Buysse, C. E., Kaulfus, A., Nair, U. and Jaffe, D. A.: Relationships between Particulate Matter,

525   Ozone, and Nitrogen Oxides during Urban Smoke Events in the Western US, Environ.

526   Sci. Technol., 53(21), 12519–12528, doi:10.1021/acs.est.9b05241, 2019.

527   Colarco, P. R., Schoeberl, M. R., Doddridge, B. G., Marufu, L. T., Torres, O. and Welton, E. J.:

528   Transport of smoke from Canadian forest fires to the surface near Washington, D.C.:

529   Injection height, entrainment, and optical properties, J. Geophys. Res. D Atmos., 109(6),

530   1–12, doi:10.1029/2003JD004248, 2004.

531   Cottle, P., Strawbridge, K. and McKendry, I.: Long-range transport of Siberian wildfire smoke to

532   British Columbia: Lidar observations and air quality impacts, Atmos. Environ.,

533   doi:10.1016/j.atmosenv.2014.03.005, 2014.

534   Davidian, J.-C. and Kopriva, S.: Regulation of Sulfate Uptake and Assimilation—the Same or

535   Not the Same?, Mol. Plant, 3(2), 314–325, doi:10.1093/MP/SSQ001, 2010.

536   DeRieux, W.-S. W., Li, Y., Lin, P., Laskin, J., Laskin, A., Bertram, A. K., Nizkorodov, S. A. and

537   Shiraiwa, M.: Predicting the glass transition temperature and viscosity of secondary

538   organic material using molecular composition, Atmos. Chem. Phys., 18(9), 6331–6351,

539   doi:10.5194/acp-18-6331-2018, 2018.

540   Ditto, J. C., Barnes, E. B., Khare, P., Takeuchi, M., Joo, T., Bui, A. A. T., Lee-Taylor, J., Eris,

541   G., Chen, Y., Aumont, B., Jimenez, J. L., Ng, N. L., Griffin, R. J. and Gentner, D. R.: An

542   omnipresent diversity and variability in the chemical composition of atmospheric

543   functionalized organic aerosol, Commun. Chem., 1(1), 75, doi:10.1038/s42004-018-

544   0074-3, 2018.

545   Ditto, J. C., Joo, T., Khare, P., Sheu, R., Takeuchi, M., Chen, Y., Xu, W., Bui, A. A. T., Sun, Y.,

546   Ng, N. L. and Gentner, D. R.: Effects of Molecular-Level Compositional Variability in

547   Organic Aerosol on Phase State and Thermodynamic Mixing Behavior, Environ. Sci.

548   Technol., 53(22), 13009–13018, doi:10.1021/acs.est.9b02664, 2019.

549   Ditto, J. C., Joo, T., Slade, J. H., Shepson, P. B., Ng, N. L. and Gentner, D. R.: Nontargeted

550    Tandem Mass Spectrometry Analysis Reveals Diversity and Variability in Aerosol

551    Functional Groups across Multiple Sites, Seasons, and Times of Day, Environ. Sci.

552    Technol. Lett., 7(2), 60–69, doi:10.1021/acs.estlett.9b00702, 2020.

553 Donahue, N. M., Epstein, S. A., Pandis, S. N. and Robinson, A. L.: A two-dimensional volatility

554    basis set: 1. organic-aerosol mixing thermodynamics, Atmos. Chem. Phys., 11(7), 3303–

555    3318, doi:10.5194/acp-11-3303-2011, 2011.

556 Dreessen, J., Sullivan, J. and Delgado, R.: Observations and impacts of transported Canadian

557    wildfire smoke on ozone and aerosol air quality in the Maryland region on June 9–12,

558    2015, J. Air Waste Manag. Assoc., 66(9), 842–862,

559    doi:10.1080/10962247.2016.1161674, 2016.

560 Duporté, G., Parshintsev, J., Barreira, L. M. F., Hartonen, K., Kulmala, M. and Riekkola, M. L.:

561    Nitrogen-Containing Low Volatile Compounds from Pinonaldehyde-Dimethylamine

562    Reaction in the Atmosphere: A Laboratory and Field Study, Environ. Sci. Technol.,

563    50(9), 4693–4700, doi:10.1021/acs.est.6b00270, 2016.

564 Duporté, G., Riva, M., Parshintsev, J., Heikkinen, E., Barreira, L. M. F., Myllys, N., Heikkinen,

565    L., Hartonen, K., Kulmala, M., Ehn, M. and Riekkola, M. L.: Chemical Characterization

566    of Gas- and Particle-Phase Products from the Ozonolysis of α-Pinene in the Presence of

567    Dimethylamine, Environ. Sci. Technol., 51(10), 5602–5610,

568    doi:10.1021/acs.est.6b06231, 2017.

569 Fenn, M. E., Bytnerowicz, A., Schilling, S. L. and Ross, C. S.: Atmospheric deposition of

570    nitrogen, sulfur and base cations in jack pine stands in the Athabasca Oil Sands Region,

571    Alberta, Canada, Environ. Pollut., 196, 497–510, doi:10.1016/j.envpol.2014.08.023,

572    2015.

Forrister, H., Liu, J., Scheuer, E., Dibb, J., Ziemba, L., Thornhill, K. L., Anderson, B., Diskin, G., Perring, A. E., Schwarz, J. P., Campuzano-Jost, P., Day, D. A., Palm, B. P., Jimenez, J. L., Nenes, A. and Weber, R. J.: Evolution of brown carbon in wildfire plumes, Geophys. Res. Lett., 42, 4623–4630, 2015.

Forster, C., Wandinger, U., Wotawa, G., James, P., Mattis, I., Althausen, D., Simmonds, P., O'Doherty, S., Jennings, S. G., Kleefeld, C., Schneider, J., Trickl, T., Kreipl, S., Jäger, H. and Stohl, A.: Transport of boreal forest fire emissions from Canada to Europe, J. Geophys. Res. Atmos., 106(D19), 22887–22906, doi:10.1029/2001JD900115, 2001.

Gahan, J. and Schmalenberger, A.: The role of bacteria and mycorrhiza in plant sulfur supply, Front. Plant Sci., 5(DEC), 1–7, doi:10.3389/fpls.2014.00723, 2014.

Garofalo, L. A., Pothier, M. A., Levin, E. J. T., Campos, T., Kreidenweis, S. M. and Farmer, D. K.: Emission and Evolution of Submicron Organic Aerosol in Smoke from Wildfires in the Western United States, ACS Earth Sp. Chem., 3(7), 1237–1247, doi:10.1021/acsearthspacechem.9b00125, 2019.

Gilman, J. B., Lerner, B. M., Kuster, W. C., Goldan, P. D., Warneke, C., Veres, P. R., Roberts, J. M., De Gouw, J. A., Burling, I. R. and Yokelson, R. J.: Biomass burning emissions and potential air quality impacts of volatile organic compounds and other trace gases from fuels common in the US, Atmos. Chem. Phys., 15(24), 13915–13938, doi:10.5194/acp-15-13915-2015, 2015.

Hallquist, M., Wenger, J. C., Baltensperger, U., Rudich, Y., Simpson, D., Claeys, M., Dommen, J., Donahue, N. M., George, C., Goldstein, A. H., Hamilton, J. F., Herrmann, H., Hoffmann, T., Iinuma, Y., Jang, M., Jenkin, M. E., Jimenez, J. L., Kiendler-Scharr, A., Maenhaut, W., McFiggans, G., Mentel, T. F., Monod, A., Prevot, A. S. H., Seinfeld, J.

596   H., Surratt, J. D., Szmigielski, R. and Wildt, J.: The formation, properties and impact of

597   secondary organic aerosol: current and emerging issues, Atmos. Chem. Phys., 9(14),

598   5155–5236, doi:10.5194/acp-9-5155-2009, 2009.

599   Hatch, L. E., Luo, W., Pankow, J. F., Yokelson, R. J., Stockwell, C. E. and Barsanti, K. C.:

600   Identification and quantification of gaseous organic compounds emitted from biomass

601   burning using two-dimensional gas chromatography-time-of-flight mass spectrometry,

602   Atmos. Chem. Phys., 15(4), 1865–1899, doi:10.5194/acp-15-1865-2015, 2015.

603   Hatch, L. E., Rivas-Ubach, A., Jen, C. N., Lipton, M., Goldstein, A. H. and Barsanti, K. C.:

604   Measurements of I/SVOCs in biomass-burning smoke using solid-phase extraction disks

605   and two-dimensional gas chromatography, Atmos. Chem. Phys., 18(24), 17801–17817,

606   doi:10.5194/acp-18-17801-2018, 2018.

607   Hatch, L. E., Jen, C. N., Kreisberg, N. M., Selimovic, V., Yokelson, R. J., Stamatis, C., York, R.

608   A., Foster, D., Stephens, S. L., Goldstein, A. H. and Barsanti, K. C.: Highly Speciated

609   Measurements of Terpenoids Emitted from Laboratory and Mixed-Conifer Forest

610   Prescribed Fires, Environ. Sci. Technol., 53(16), 9418–9428,

611   doi:10.1021/acs.est.9b02612, 2019.

612   Hecobian, A., Liu, Z., Hennigan, C. J., Huey, L. G., Jimenez, J. L., Cubison, M. J., Vay, S.,

613   Diskin, G. S., Sachse, G. W., Wisthaler, A., Mikoviny, T., Weinheimer, A. J., Liao, J.,

614   Knapp, D. J., Wennberg, P. O., Kürten, A., Crounse, J. D., St. Clair, J., Wang, Y. and

615   Weber, R. J.: Comparison of chemical characteristics of 495 biomass burning plumes

616   intercepted by the NASA DC-8 aircraft during the ARCTAS/CARB-2008 field

617   campaign, Atmos. Chem. Phys., 11(24), 13325–13337, doi:10.5194/acp-11-13325-2011,

618   2011.

619   Hegg, D. A., Radke, L. F., Hobbs, P. V. and Brock, C. A.: Nitrogen and Sulfur Emissions From

620   The Burning of Forest Products Near Large Urban Areas, J. Geophys. Res., 92, 701–714,

621   1987.

622   Hennigan, C. J., Miracolo, M. A., Engelhart, G. J., May, A. A., Presto, A. A., Lee, T., Sullivan,

623   A. P., McMeeking, G. R., Coe, H., Wold, C. E., Hao, W. M., Gilman, J. B., Kuster, W.

624   C., De Gouw, J., Schichtel, B. A., Collett, J. L., Kreidenweis, S. M. and Robinson, A. L.:

625   Chemical and physical transformations of organic aerosol from the photo-oxidation of

626   open biomass burning emissions in an environmental chamber, Atmos. Chem. Phys.,

627   11(15), 7669–7686, doi:10.5194/acp-11-7669-2011, 2011.

628   Huang, W. Z. and Schoenau, J. J.: Forms, amounts and distribution of carbon, nitrogen,

629   phosphorus and sulfur in a boreal aspen forest soil, Can. J. Soil Sci., 76(3), 373–385,

630   doi:10.4141/cjss96-045, 1996.

631   Iinuma, Y., Böge, O. and Herrmann, H.: Methyl-nitrocatechols: Atmospheric tracer compounds

632   for biomass burning secondary organic aerosols, Environ. Sci. Technol., 44(22), 8453–

633   8459, doi:10.1021/es102938a, 2010.

634   Jencks, W. P. and Lienhard, G. E.: Thiol Addition to the Carbonyl Group. Equilibria and

635   Kinetics, J. Am. Chem. Soc., 88(17), 3982–3995, doi:10.1021/ja00969a017, 1966.

636   Jiang, H., Frie, A. L., Lavi, A., Chen, J. Y., Zhang, H., Bahreini, R. and Lin, Y. H.: Brown

637   Carbon Formation from Nighttime Chemistry of Unsaturated Heterocyclic Volatile

638   Organic Compounds, Environ. Sci. Technol. Lett., 6(3), 184–190,

639   doi:10.1021/acs.estlett.9b00017, 2019.

640   Jolly, W. M., Cochrane, M. A., Freeborn, P. H., Holden, Z. A., Brown, T. J., Williamson, G. J.

641   and Bowman, D. M. J. S.: Climate-induced variations in global wildfire danger from

642   1979 to 2013, Nat. Commun., 6(May), 1–11, doi:10.1038/ncomms8537, 2015.

643   Khare, P., Marcotte, A., Sheu, R., Walsh, A. N., Ditto, J. C. and Gentner, D. R.: Advances in

644   offline approaches for trace measurements of complex organic compound mixtures via

645   soft ionization and high-resolution tandem mass spectrometry, J. Chromatogr. A, 1598,

646   163–174, doi:10.1016/j.chroma.2019.03.037, 2019.

647   Koss, A. R., Sekimoto, K., Gilman, J. B., Selimovic, V., Coggon, M. M., Zarzana, K. J., Yuan,

648   B., Lerner, B. M., Brown, S. S., Jimenez, J. L., Krechmer, J., Roberts, J. M., Warneke,

649   C., Yokelson, R. J. and De Gouw, J.: Non-methane organic gas emissions from biomass

650   burning: Identification, quantification, and emission factors from PTR-ToF during the

651   FIREX 2016 laboratory experiment, Atmos. Chem. Phys., 18(5), 3299–3319,

652   doi:10.5194/acp-18-3299-2018, 2018.

653   Van Krevelen, D. W. and Te Nijenhuis, K.: Properties of Polymers, 4th ed., Elsevier,

654   Amsterdam., 2009.

655   Landis, M. S., Edgerton, E. S., White, E. M., Wentworth, G. R., Sullivan, A. P. and Dillner, A.

656   M.: The impact of the 2016 Fort McMurray Horse River Wildfire on ambient air

657   pollution levels in the Athabasca Oil Sands Region, Alberta, Canada, Sci. Total Environ.,

658   618, 1665–1676, doi:10.1016/j.scitotenv.2017.10.008, 2018.

659   Laskin, A., Smith, J. S. and Laskin, J.: Molecular Characterization of Nitrogen-Containing

660   Organic Compounds in Biomass Burning Aerosols Using High-Resolution Mass

661   Spectrometry, Environ. Sci. Technol., 43(10), 3764–3771, doi:10.1021/es803456n, 2009.

662   Leustek, T.: Sulfate Metabolism, Arab. B., 1(e0017), 1–16, doi:10.1199/tab.0017, 2002.

663   Li, S. M., Leithead, A., Moussa, S. G., Liggio, J., Moran, M. D., Wang, D., Hayden, K.,

664   Darlington, A., Gordon, M., Staebler, R., Makar, P. A., Stroud, C. A., McLaren, R., Liu,

665   P. S. K., O'Brien, J., Mittermeier, R. L., Zhang, J., Marson, G., Cober, S. G., Wolde, M.

666   and Wentzell, J. J. B.: Differences between measured and reported volatile organic

667   compound emissions from oil sands facilities in Alberta, Canada, Proc. Natl. Acad. Sci.

668   U. S. A., 114(19), E3756–E3765, doi:10.1073/pnas.1617862114, 2017.

669 Li, Y., Pöschl, U. and Shiraiwa, M.: Molecular corridors and parameterizations of volatility in

670   the chemical evolution of organic aerosols, Atmos. Chem. Phys., 16(5), 3327–3344,

671   doi:10.5194/acp-16-3327-2016, 2016.

672 Liggio, J., Li, S.-M., Hayden, K., Taha, Y. M., Stroud, C., Darlington, A., Drollette, B. D.,

673   Gordon, M., Lee, P., Liu, P., Leithead, A., Moussa, S. G., Wang, D., OBrien, J.,

674   Mittermeier, R. L., Brook, J. R., Lu, G., Staebler, R. M., Han, Y., Tokarek, T. W.,

675   Osthoff, H. D., Makar, P. A., Zhang, J., Plata, D. L. and Gentner, D. R.: Oil sands

676   operations as a large source of secondary organic aerosols, Nature, 534,

677   doi:10.1038/nature17646, 2016.

678 Liggio, J., Moussa, S. G., Wentzell, J., Darlington, A., Liu, P., Leithead, A., Hayden, K., OBrien,

679   J., Mittermeier, R. L., Staebler, R., Wolde, M. and Li, S. M.: Understanding the primary

680   emissions and secondary formation of gaseous organic acids in the oil sands region of

681   Alberta, Canada, Atmos. Chem. Phys., 17(13), 8411–8427, doi:10.5194/acp-17-8411-

682   2017, 2017.

683 Lim, C. Y., Hagan, D. H., Coggon, M. M., Koss, A. R., Sekimoto, K., De Gouw, J., Warneke,

684   C., Cappa, C. D. and Kroll, J. H.: Secondary organic aerosol formation from the

685   laboratory oxidation of biomass burning emissions, Atmos. Chem. Phys., 19(19), 12797–

686   12809, doi:10.5194/acp-19-12797-2019, 2019.

687 Lin, P., Yu, J. Z., Engling, G. and Kalberer, M.: Organosulfates in humic-like substance fraction

688   isolated from aerosols at seven locations in East Asia: A study by ultra-high-resolution

689   mass spectrometry, Environ. Sci. Technol., 46(24), 13118–13127,

690   doi:10.1021/es303570v, 2012.

691 Lin, P., Fleming, L. T., Nizkorodov, S. A., Laskin, J. and Laskin, A.: Comprehensive Molecular

692   Characterization of Atmospheric Brown Carbon by High Resolution Mass Spectrometry

693   with Electrospray and Atmospheric Pressure Photoionization, Anal. Chem., 90(21),

694   12493–12502, doi:10.1021/acs.analchem.8b02177, 2018.

695 Liu, J. C., Wilson, A., Mickley, L. J., Dominici, F., Ebisu, K., Wang, Y., Sulprizio, M. P., Peng,

696   R. D., Yue, X., Son, J.-Y., Anderson, G. B. and Bell, M. L.: Wildfire-specific Fine

697   Particulate Matter and Risk of Hospital Admissions in Urban and Rural Counties,

698   Epidemiology, 28(1), 77–85, doi:10.1111/mec.13536.Application, 2017.

699 Liu, Y., Liggio, J. and Staebler, R.: Reactive uptake of ammonia to secondary organic aerosols:

700   Kinetics of organonitrogen formation, Atmos. Chem. Phys., 15(23), 13569–13584,

701   doi:10.5194/acp-15-13569-2015, 2015.

702 Di Lorenzo, R. A., Place, B. K., VandenBoer, T. C. and Young, C. J.: Composition of Size-

703   Resolved Aged Boreal Fire Aerosols: Brown Carbon, Biomass Burning Tracers, and

704   Reduced Nitrogen, ACS Earth Sp. Chem., 2(3), 278–285,

705   doi:10.1021/acsearthspacechem.7b00137, 2018.

706 Lowe, A. B.: Thiol-ene "click" reactions and recent applications in polymer and materials

707   synthesis, Polym. Chem., 1(1), 17–36, doi:10.1039/b9py00216b, 2010.

708 Makar, P. A., Akingunola, A., Aherne, J., Cole, A. S., Aklilu, Y. A., Zhang, J., Wong, I.,

709   Hayden, K., Li, S. M., Kirk, J., Scott, K., Moran, M. D., Robichaud, A., Cathcart, H.,

710   Baratzedah, P., Pabla, B., Cheung, P., Zheng, Q. and Jeffries, D. S.: Estimates of

711   exceedances of critical loads for acidifying deposition in Alberta and Saskatchewan,

712   Atmos. Chem. Phys., 18(13), 9897–9927, doi:10.5194/acp-18-9897-2018, 2018.

713   Mashkina, A. V.: Catalytic Synthesis Of Sulfides Sulfoxides and Sulfones, Sulfur reports, 10(4),

714   279–388, doi:10.1080/01961779108048759, 1991.

715   McLinden, C. A., Fioletov, V., Krotkov, N. A., Li, C., Boersma, K. F. and Adams, C.: A Decade

716   of Change in NO2 and SO2 over the Canadian Oil Sands As Seen from Space, Environ.

717   Sci. Technol., 50(1), 331–337, doi:10.1021/acs.est.5b04985, 2016.

718   Meng, F. R., Bourque, C. P. A., Belczewski, R. F., Whitney, N. J. and Arp, P. A.: Foliage

719   responses of spruce trees to long-term low-grade sulfur dioxide deposition, Environ.

720   Pollut., 90(2), 143–152, doi:10.1016/0269-7491(94)00101-I, 1995.

721   Murphy, B. N., Donahue, N. M., Robinson, A. L. and Pandis, S. N.: A naming convention for

722   atmospheric organic aerosol, Atmos. Chem. Phys., 14(11), 5825–5839, doi:10.5194/acp-

723   14-5825-2014, 2014.

724   Nozière, B., Kalberer, M., Claeys, M., Allan, J., D'Anna, B., Decesari, S., Finessi, E., Glasius,

725   M., Grgić, I., Hamilton, J. F., Hoffmann, T., Iinuma, Y., Jaoui, M., Kahnt, A., Kampf, C.

726   J., Kourtchev, I., Maenhaut, W., Marsden, N., Saarikoski, S., Schnelle-Kreis, J., Surratt,

727   J. D., Szidat, S., Szmigielski, R. and Wisthaler, A.: The Molecular Identification of

728   Organic Compounds in the Atmosphere: State of the Art and Challenges, Chem. Rev.,

729   115(10), 3919–3983, doi:10.1021/cr5003485, 2015.

730   Nyborg, M., Solberg, E. D., Malhi, S. S., Takyi, S., Yeung, P. and Chaudhry, M.: Deposition of

731   anthropogenic sulphur dioxide on soils and resulting soil acidification, Plant-Soil Interact.

732   Low pH, 147–156, doi:10.1007/978-94-011-3438-5_16, 1991.

733   Onda, Y.: Oxidative protein-folding systems in plant cells, Int. J. Cell Biol., 2013,

734   doi:10.1155/2013/585431, 2013.

735   Pan, Y. P., Wang, Y. S., Tang, G. Q. and Wu, D.: Spatial distribution and temporal variations of

736   atmospheric sulfur deposition in Northern China: Insights into the potential acidification

737   risks, Atmos. Chem. Phys., 13(3), 1675–1688, doi:10.5194/acp-13-1675-2013, 2013.

738   Reid, C. E., Brauer, M., Johnston, F. H., Jerrett, M., Balmes, J. R. and Elliott, C. T.: Critical

739   review of health impacts of wildfire smoke exposure, Environ. Health Perspect., 124(9),

740   1334–1343, doi:10.1289/ehp.1409277, 2016.

741   Rogers, H. M., Ditto, J. C. and Gentner, D. R.: Evidence for impacts on surface-level air quality

742   in the northeastern US from long-distance transport of smoke from North American fires

743   during the Long Island Sound Tropospheric Ozone Study (LISTOS) 2018, Atmos. Chem.

744   Phys., 20(2), 671–682, doi:10.5194/acp-20-671-2020, 2020.

745   Sekimoto, K., Koss, A. R., Gilman, J. B., Selimovic, V., Coggon, M. M., Zarzana, K. J., Yuan,

746   B., Lerner, B. M., Brown, S. S., Warneke, C., Yokelson, R. J., Roberts, J. M. and De

747   Gouw, J.: High-and low-temperature pyrolysis profiles describe volatile organic

748   compound emissions from western US wildfire fuels, Atmos. Chem. Phys., 18(13),

749   9263–9281, doi:10.5194/acp-18-9263-2018, 2018.

750   Sengupta, D., Samburova, V., Bhattarai, C., Kirillova, E., Mazzoleni, L., Iaukea-Lum, M., Watts,

751   A., Moosmüller, H. and Khlystov, A.: Light absorption by polar and non-polar aerosol

752   compounds from laboratory biomass combustion, Atmos. Chem. Phys., 18(15), 10849–

753   10867, doi:10.5194/acp-18-10849-2018, 2018.

754   Sheu, R., Marcotte, A., Khare, P., Charan, S., Ditto, J. C. and Gentner, D. R.: Advances in

755   offline approaches for chemically speciated measurements of trace gas-phase organic

756   compounds via adsorbent tubes in an integrated sampling-to-analysis system, J.

757   Chromatogr. A, 1575, 80–90, doi:10.1016/j.chroma.2018.09.014, 2018.

758   Song, J., Li, M., Fan, X., Zou, C., Zhu, M., Jiang, B., Yu, Z., Jia, W., Liao, Y. and Peng, P.:

759   Molecular Characterization of Water- And Methanol-Soluble Organic Compounds

760   Emitted from Residential Coal Combustion Using Ultrahigh-Resolution Electrospray

761   Ionization Fourier Transform Ion Cyclotron Resonance Mass Spectrometry, Environ. Sci.

762   Technol., 53(23), 13607–13617, doi:10.1021/acs.est.9b04331, 2019.

763   Updyke, K. M., Nguyen, T. B. and Nizkorodov, S. A.: Formation of brown carbon via reactions

764   of ammonia with secondary organic aerosols from biogenic and anthropogenic

765   precursors, Atmos. Environ., 63, 22–31, doi:10.1016/j.atmosenv.2012.09.012, 2012.

766   Val Martín, M., Honrath, R. E., Owen, R. C., Pfister, G., Fialho, P. and Barata, F.: Significant

767   enhancements of nitrogen oxides, black carbon, and ozone in the North Atlantic lower

768   free troposphere resulting from North American boreal wildfires, J. Geophys. Res.

769   Atmos., 111(23), 1–17, doi:10.1029/2006JD007530, 2006.

770   Vicente, A., Alves, C., Calvo, A. I., Fernandes, A. P., Nunes, T., Monteiro, C., Almeida, S. M.

771   and Pio, C.: Emission factors and detailed chemical composition of smoke particles from

772   the 2010 wildfire season, Atmos. Environ., doi:10.1016/j.atmosenv.2013.01.062, 2013.

773   Wang, X., Wang, H., Jing, H., Wang, W. N., Cui, W., Williams, B. J. and Biswas, P.: Formation

774   of Nitrogen-Containing Organic Aerosol during Combustion of High-Sulfur-Content

775   Coal, Energy and Fuels, 31(12), 14161–14168, doi:10.1021/acs.energyfuels.7b02273,

776   2017a.

777   Wang, X. K., Rossignol, S., Ma, Y., Yao, L., Wang, M. Y., Chen, J. M., George, C. and Wang,

778   L.: Molecular characterization of atmospheric particulate organosulfates in three

779   megacities at the middle and lower reaches of the Yangtze River, Atmos. Chem. Phys.,

780   16(4), 2285–2298, doi:10.5194/acp-16-2285-2016, 2016.

781   Wang, X. K., Hayeck, N., Brüggemann, M., Yao, L., Chen, H., Zhang, C., Emmelin, C., Chen,

782   J., George, C. and Wang, L.: Chemical Characteristics of Organic Aerosols in Shanghai:

783   A Study by Ultrahigh-Performance Liquid Chromatography Coupled With Orbitrap Mass

784   Spectrometry, J. Geophys. Res. Atmos., 122(21), 11,703-11,722,

785   doi:10.1002/2017JD026930, 2017b.

786   Ward, D. E.: Factors Influencing the Emissions of Gases and Particulate Matter from Biomass

787   Burning, in Fire in the Tropical Biota: Ecosystem Processes and Global Challenges, pp.

788   418–436., 1990.

789   Wong, J. P. S., Tsagkaraki, M., Tsiodra, I., Mihalopoulos, N., Violaki, K., Kanakidou, M.,

790   Sciare, J., Nenes, A. and Weber, R. J.: Effects of Atmospheric Processing on the

791   Oxidative Potential of Biomass Burning Organic Aerosols, Environ. Sci. Technol.,

792   53(12), 6747–6756, doi:10.1021/acs.est.9b01034, 2019.

793   Yokelson, R. J., Burling, I. R., Gilman, J. B., Warneke, C., Stockwell, C. E., De Gouw, J., Akagi,

794   S. K., Urbanski, S. P., Veres, P., Roberts, J. M., Kuster, W. C., Reardon, J., Griffith, D.

795   W. T., Johnson, T. J., Hosseini, S., Miller, J. W., Cocker, D. R., Jung, H. and Weise, D.

796   R.: Coupling field and laboratory measurements to estimate the emission factors of

797   identified and unidentified trace gases for prescribed fires, Atmos. Chem. Phys., 13(1),

798   89–116, doi:10.5194/acp-13-89-2013, 2013.
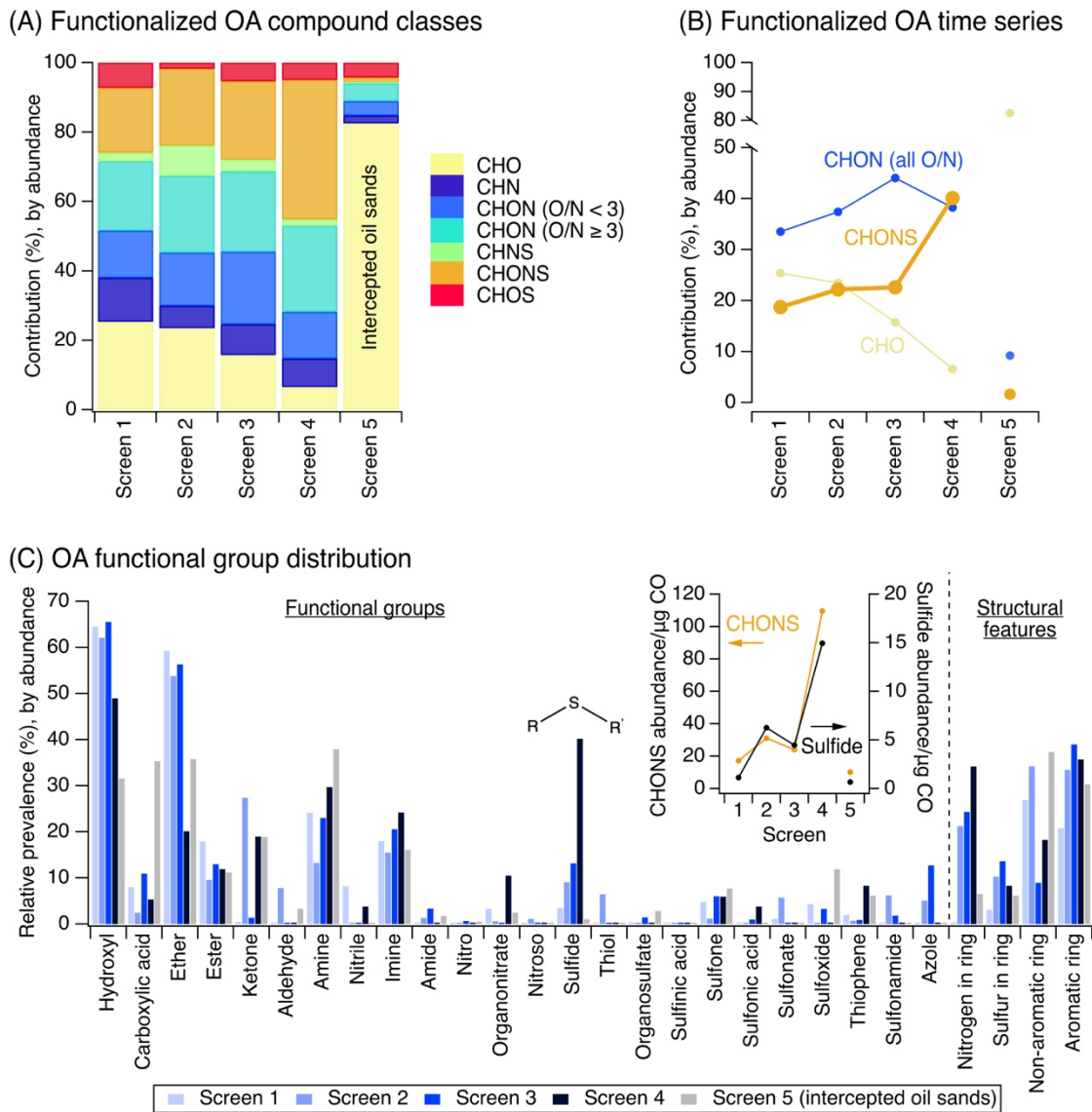
Figure 1. (A) The compound class distribution of functionalized OA (from non-targeted LC-ESI-MS) weighted by ion abundance, shown as percent contribution of each compound class to the total compound abundance measured by LC-ESI-MS. (B) Percent contribution of CHO, CHON, and CHONS compound classes in functionalized OA as a function of plume age. CHON compounds in panel B are summed across all O/N ratios. (C) Functional groups and structural features present in measured functionalized OA (from non-targeted LC-ESI-MS/MS). The sulfide functional group is shown here for emphasis, and will be the subject of subsequent analyses. The inset in panel C shows the absolute CHONS ion abundance normalized by CO mass (orange trace, left y-axis) and the absolute sulfide ion abundance normalized by CO mass (black trace, right y-axis). Full CO-adjusted compound class and functional group abundance data are shown in Figures S5-S6. For panels A-C, results tabulated by occurrence are also shown in Figure S5-S6.
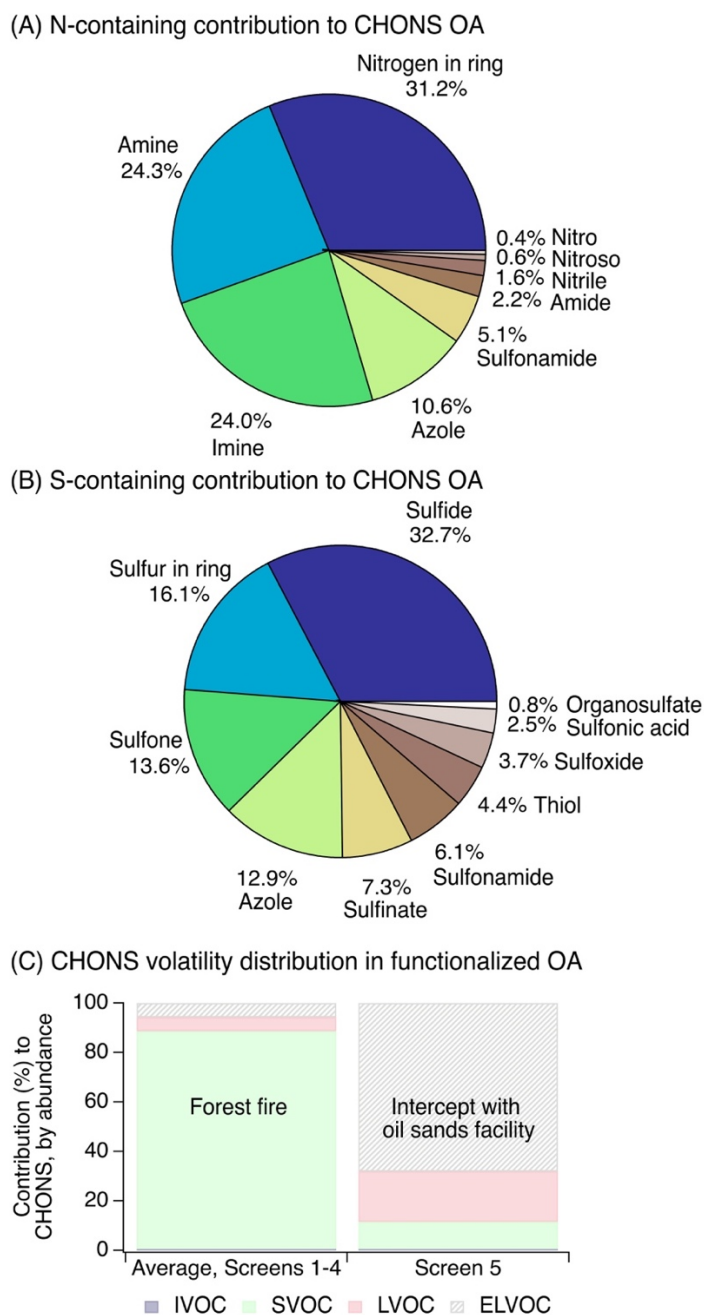
Figure 2. (A) The distribution of nitrogen-containing functional groups to particle-phase CHONS compounds (organonitrates are excluded here due to challenges with their identification using SIRIUS with CSI:FingerID, but contributed minimally to CHONS, Supporting Information S3). (B) The distribution of sulfur-containing groups to particle-phase CHONS compounds. For panels A-B, data are averaged across screens 1-4, with individual screens shown in Figure S7A. (C) Volatility distribution of particle-phase CHONS species. These volatility data were averaged across screens 1-4, and individual screens are shown in Figure S8. Volatility was estimated with the parameterization in Li et al. (Li et al., 2016) and grouped according to volatility bins in Donahue et al. (Donahue et al., 2011).
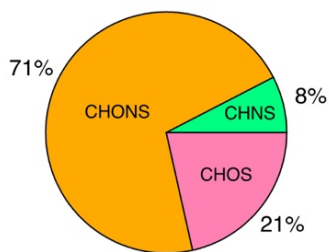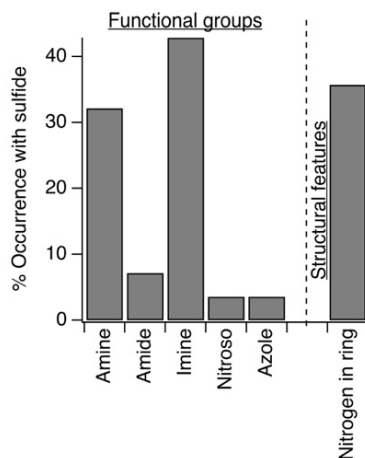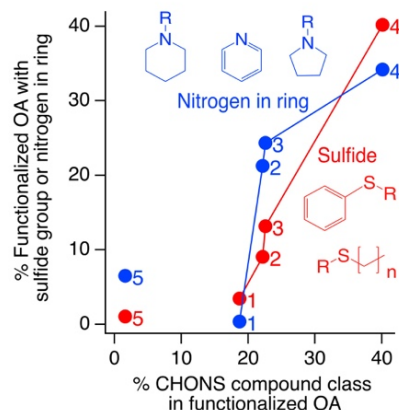
Figure 3. (A) Compound class distribution of sulfide groups: 71% of sulfide functional groups observed (weighted by ion abundance) were present in CHONS compounds. (B) Co-occurrence of sulfides and nitrogen-containing groups. Data shown in panels A-B are cumulative across compounds in screens 1-4. (C) The relative contribution of sulfides and cyclic nitrogen groups to all functionalized OA increased together with the increasing contribution of CHONS compounds. The other functional groups in panel B showed no relationship with the increase in CHONS (Figure S7B). Structures represent examples of commonly observed sulfide and cyclic nitrogen substructures from SIRIUS and CSI:FingerID (Supporting Information S3), where ring structures associated with nitrogen heteroatoms were free standing, adjacent to other rings, and/or contained additional attached functional groups.

(A) Average gas-phase $C_xH_yS_1$ distribution
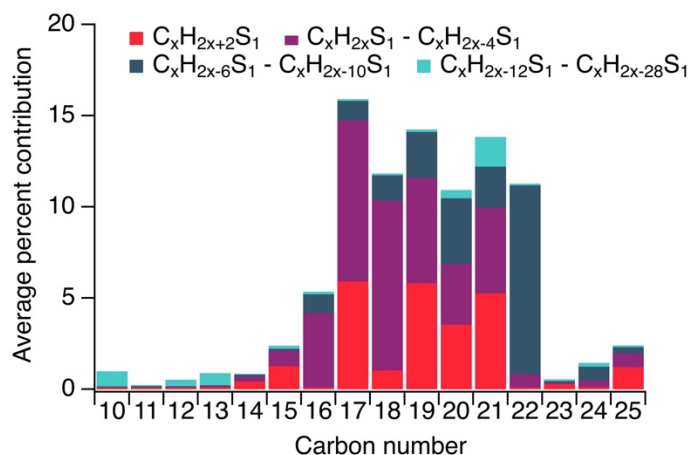
(B) Gas-phase and AMS OA concentrations normalized by CO
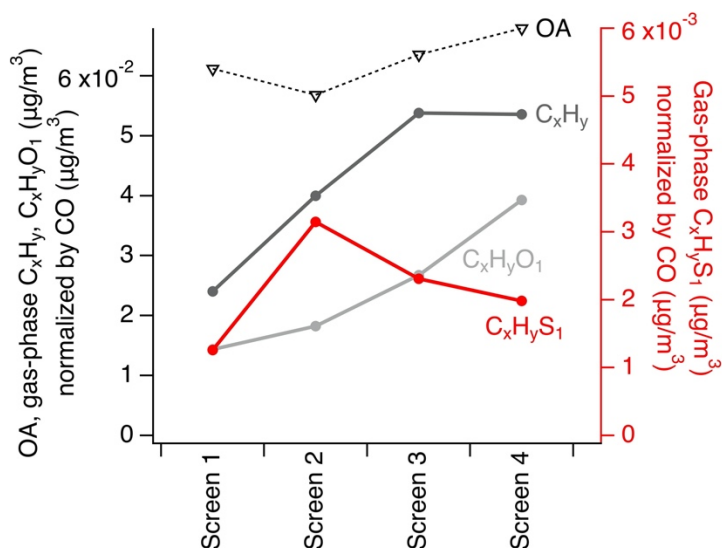
Figure 4. (A) The average $C_xH_yS_1$ distribution from targeted GC-APCI-MS across all gas-phase adsorbent tube samples from screens 1-4 (see Figure S10 for individual $C_xH_yS_1$ screens, and Figure S13 for C_xH_y). (B) Concentrations of gas-phase C_xH_y, $C_xH_yO_1$, $C_xH_yS_1$ from targeted GC-APCI-MS analysis of adsorbent tubes, shown with total OA from AMS, all corrected for dilution using carbon monoxide measurements (see Figure S12A for non-normalized concentrations). Data in panel B are averaged over low and high altitude adsorbent tube samples.